An Efficient Surface Smoothing Method for Microstructures Based on Vibration-assisted Digital Grayscale Lithography

Shengzhou Huang[1,2,3], Bowen Ren[2], Chengwei Jiang[2], Fanglin Xie[*2], Yuanzhuo Tang[2], Zhaowei Tian[2], Jinjin Huang[4], and Zhi Li[5]

[1]*School of Artificial Intelligence, Anhui Polytechnic University, Wuhu 241000, China*
[2]*School of Mechanical Engineering, Anhui Polytechnic University, Wuhu 241000, China*
[3]*Anhui East China Photoelectric Technology Research Institute, Wuhu 241002, China*
[4]*Wuhu Changpeng Parts Co., LTD, Wuhu 241002, China*
[5]*Hefei core Acer Microelectronics Equipment Co., LTD, Hefei 230000, China*
**Corresponding author's e-mail: 019172@ahpu.edu.cn*

In this paper, an efficient surface smoothing method for improving the microstructure quality was proposed. A mechanical vibration-assisted smoothing microstructures surface strategy based on maskless grayscale lithography of digital micromirror device (DMD) was developed, which can effectively improve the microstructures surface quality and alleviate the effects of DMD pixel quantization errors. The experimental results showed that the micro-lens array microstructure surface roughness was reduced from 1.657 μm to 0.207 μm by the above strategy. The proposed method will have great potential for application in the field of micro-optical components high efficiency and high precision manufacturing.

DOI: 10.2961/jlmn.2024.02.2004
Keywords: digital micromirror device (DMD), vibration-assisted, digital grayscale lithography, microstructures, surface smoothing

1.Introduction

With the escalating demand for the miniaturization of optoelectronic devices, the micro-lens array microstructure has become a crucial miniature optical device, characterized by a high surface finish and superior optical performance [1]. This device is widely utilized in compact imaging [2,3], sensing [4,5], biomedical [6-8], 3D display [9-12], photovoltaic [13, 14], and other fields. Currently, methods for fabricating micro-lens structures, such as photoresist thermal reflow [15], micro-drop injection [11,16], and laser direct writing [17,18], are challenging to balance efficiency and cost, and are plagued by lengthy processing times, high process complexity, and difficulty in maintaining consistency. Digital lithography, based on a digital micromirror device (DMD), offers benefits such as high processing efficiency, low-cost, and excellent flexibility [19-21]. This technology has garnered significant attention from scholars in recent years, and is considered a new digital lithography technology, following the single dot laser direct writing technology.

However, due to the structural characteristics of DMD, there is a 1 μm gap between each micromirror. When the digital mask is displayed on the DMD, the device will sample and quantize the digital mask based on the pixel size. The pixels of the mask graphics are not all integer multiples, leading to non-integer pixel quantization errors in the lithography process. This results in discrete pixels, which can generate dark grids, leading to rough micro-lens surfaces. To address this issue, scholars at home and abroad have employed various methods. These include using high magnification objectives [22, 23], graphic staggered overlay exposures, DMD oblique scanning lithography [24-26], or designing DMD pixel integer masks and linear staggered imaging of micromirror arrays [27-29]. These methods have been employed to improve lithography resolution and consequently reduce pixel quantization errors. While these methods have improved the resolution of DMD digital lithography to varying degrees, they have not eliminated the quantization error of DMD pixels. Instead, they have reduced the size of the gap between DMD discrete pixels to varying degrees, making it challenging to achieve a smooth surface microstructure.

In this paper, we propose a mechanical vibration-assisted method, based on the mechanism of DMD pixel quantization errors. The impact of pixel quantization errors is mitigated by applying periodic vibrations to the projection objective and smearing the DMD discrete pixels. To determine the optimal vibration parameters, a theoretical simulation was initially conducted. Based on the simulation data, the optimal vibration parameters were analyzed and determined. Subsequently, a vibration-assisted digital lithography system was designed and constructed, which was subsequently experimentally verified. The results demonstrated that this method effectively enhances the surface quality of micro-lens array structures.

2. Design of vibration-assisted digital lithography system

2.1. Lithography system design

Fig.1 shows the basic components of the vibration-assisted digital grayscale lithography system schematically. Fig.1(a) shows the schematic diagram of the grayscale lithography system, which consists of five components: illumination system, DMD graphics control system, projection imaging system, precise stage motion control system and mechanical vibration assistance system. In the illumination system, the control strategy of light source synchronization is adopted. It is composed of UV-LED chip, LED constant current driver, pulse width modulation (PWM) generator, DMD chip and DMD control board. The working frequency of PWM generator is above 10KHZ, and the exposure brightness of light source can be adjusted by adjusting the duty cycle. As a spatial light modulator, DMD can realize the dynamic update of the exposure graph data, and control the on-off of the exposure light source through the real-time update data, that is, only when the graph is displayed, the signal switch of PWM generator will be opened. In the DMD graphics control system, the model of DLP 6500 (Texas Instruments, Texas, USA) was utilized with a resolution of 1920×1080, a single micromirror size of 7.56 μm and a micromirror gap of 1 μm. In the

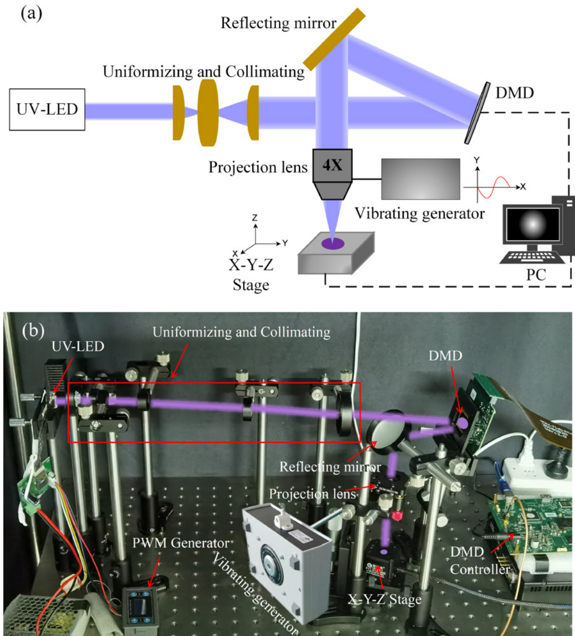

Fig. 1 Schematic diagram of the basic components of a vibration-assisted digital grayscale lithography system. (a) Schematic diagram of the system. (b) Physical diagram of the system.

projection imaging system, a flat-field achromatic objective lens (Olympus, PLN4X) was utilized to project on the photoresist substrate, which can effectively reduce the image aberration. In the precise stage motion control system, a precise piezoelectric stage (Coremorrow, *XYZ*100, E70.D3S closed loop piezoelectric controller) was adopted, which can effectively ensure the accuracy of exposure. In the mechanical vibration assistance system, it is consisting of vibration generator (Mode U56001, 3B Scientific, Germany), function generator (Mode FG100-1009956, 3B Scientific, Germany).

The mechanical vibration-assisted digital grayscale lithography systems work on the following principles. Initially, a 405 nm UV-LED light source emits an ultraviolet beam, which is then homogenized by a homogenizing collimating element. This beam is subsequently irradiated onto the DMD surface. Simultaneously, the target graphic information, which has been designed in advance, is uploaded to the DMD controller by the computer. The light beam is then reflected by the DMD to form a real-time dynamic virtual mask graphic. This graphic is scaled through the projection objective and subsequently arrives at the 3D precise motion stage. The photosensitive resin (Water Washable Resin, eSUN, Shen Zhen, China) used in the experiment is cured by the polymerization reaction under the influence of UV light [30, 31]. In the process of water washing, the unexposed photosensitive resin will be dissolved in the water, and the final cured photosensitive resin is retained to complete the engraving of the graphics. Fig.1(b) shows the physical diagram of the built vibration-assisted digital lithography system. According to the Rayleigh criterion, the system imaging resolution of 2.03 μm, and the actual minimum resolution of the system measured experimentally is 4.56 μm measured by optical microscope (DC3000, Jiangnan Yongxin Optical Co., LTD). In the process of measurement, the measurement accuracy is improved by averaging multiple samples.

2.2. DMD pixel quantization error

The occurrence of pixel quantization errors is shown in Fig. 2. *Tx* and *Ty* are the width and length of the watch mask, respectively. And *Wx* and *Wy* represent the width and length of DMD pixels, respectively. According to the principle of DMD pixel sampling, it

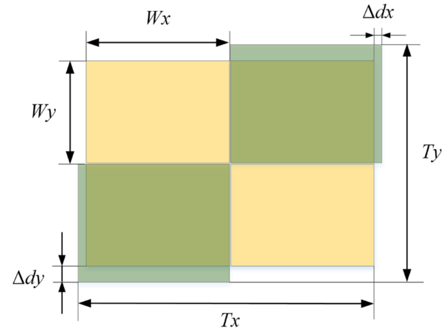

Fig. 2 The diagram of DMD pixel quantization error.

$$\frac{T_x}{2} \geq W_x, \quad \frac{T_y}{2} \geq W_y \tag{1}$$

can be represented as follows.

Since there is a certain deviation between the DMD pixel size and the mask size, the DMD pixel error should be considered when designing the mask size, and the error can be expressed by the following formula.

$$\Delta d = 2\Delta d_x \times 2\Delta d_y = \left[\mathrm{mod}(\frac{T_x}{W_x})/B\right] \times \left[\mathrm{mod}(\frac{T_y}{W_y})/B\right] \tag{2}$$

where *B* represents the zoom ratio of the projection objective.

2.3. Simulation of the influence of mechanical vibration on lithography system

The technical route of the specific method of applying vibration to the projection objective is as follows. Firstly, Abaqus finite element analysis (FEA) software was used for theoretical simulation to study the effect of periodic sinusoidal mechanical vibration on DMD lithography quality, so as to determine the optimal vibration frequency-amplitude parameters as the initial experimental parameters. Next, the experimental verification is carried out by digital gray-scale lithography system. The specific experimental process is as follows: A micro-lens digital mask consisting of 256 rings of grayscale from 0-255 is produced; After inputting the digital mask version information into the DMD, the DMD is switched on via the DMD graphics control software. Since the DMD maskless lithography system is designed with the light source pre-linked to the DMD switch, the UV-LED light source is switched on at the same time as the DMD is switched on; Finally, the vibration generator is switched on to cause the projection objective to move periodically to coat the discrete pixels according to a set function; After exposure, the substrate is washed and dried and the surface quality of the micro-lens is measured. If the results are not very good, further vibration parameter adjustment and optimization can be carried out to obtain the best combination of vibration parameters.

The influence of the vibration direction of different projection objectives on the image quality is studied by finite element simulation, that is, the unidirectional vibration direction and the diagonal vibration direction relative to the projection region, as shown in Fig. 3. From Fig.3(a) and 3(c), it is evident that the unidirectional vibration has an uneven impact on the X and Y directional displacements. Furthermore, the diagonal vibration can simultaneously affect discrete pixels in the X and Y directions. Fig.3(b) and 3(d) were the effects of different frequencies and amplitudes on the displacements, respectively. The results showed that the frequency has a great influence on the displacement. When the frequency is close to 160 Hz, the *X* and *Y* displacement are 0.23 μm, and the displacement size just covers the DMD micromirror gap, which provides a reference for the next experimental parameter setting. Here, it should be noted that in

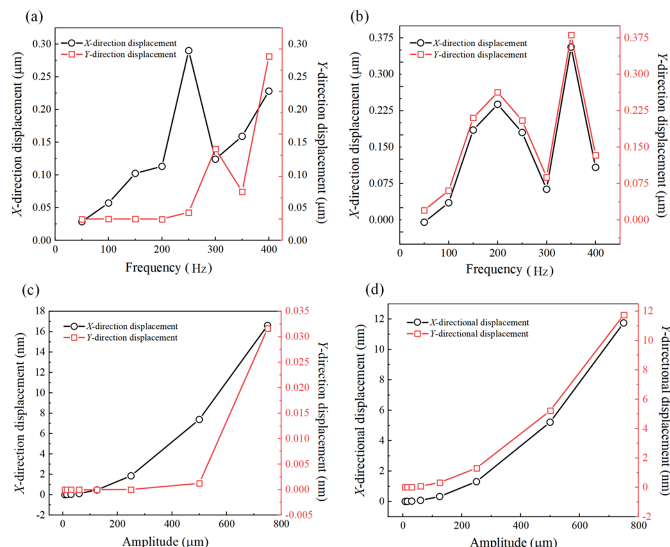

Fig. 3 Simulation of mechanical vibration acting on projection objective. (a) Unidirectional vibration, effect of frequency on displacement. (b) Diagonal vibration, effect of frequency on displacement. (c) Unidirectional vibration, effect of amplitude on displacement. (d) Diagonal vibration, effect of amplitude on displacement.

Fig.3(a) and 3(b), the ordinate *X*/*Y* displacement unit is micron. Although there are fluctuations, the difference is very small, and the maximum fluctuation is not more than 100 nm. This irregular fluctuation may be caused by the interaction of many factors in the system, such as the resonance effect of the system vibration frequency and the nonlinear response of the system. The main purpose of this simulation study is to show that diagonal vibration is significantly better than unidirectional vibration. The simulation results illustrate the effect of mechanical vibration on the exposure pattern, serving as a guide for uncovering the mechanism of vibration-assisted digital lithography-based DMD pixel quantization error elimination.

The change of surface quality of micro-lens before and after vibration was further quantitatively characterized by experimental verification. During the lithography process, the unidirectional linear motion of the vibration generator driving rod is firmly connected to the projection objective. The projection objective is controlled by the function generator, and the sinusoidal function mode is selected to drive the projection objective to control the projection UV pattern. The vibration is carried out in a diagonal direction along the projection area. According to the simulation results, it is obvious that the amplitude parameter of the vibration generator has a minimal impact on the results. The experimental verification has also been conducted, which demonstrates that the influence of amplitude on the roughness and shape of the micro-lens is negligible. Therefore, the amplitude was set at 1V.

3. Experimental verification

To verify the influence of the vibration direction mentioned in the simulation on the experimental results, the lithography experiments of unidirectional vibration and diagonal vibration were carried out, as shown in Fig.4. It's obviously from the Fig.4(a) and 4(b), the distortion of unidirectional (*X*/*Y*) vibration is the largest, while thedistortion of diagonal vibration is the smallest shown in Fig.4(d), which is closest to the original no vibration experimental data in Fig.4(c). Moreover, the experimental results are also consistent with the previous simulation results. The distortion mentioned in this paper refers to the distortion of the exposure pattern under the action of

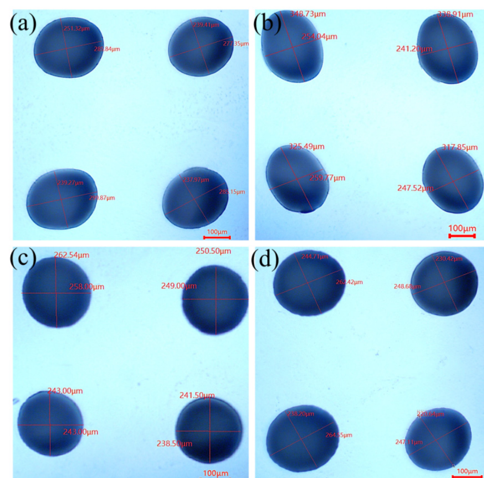

Fig. 4 The experimental results of both unidirectional vibration and diagonal vibration. (a) X direction; (b) Y direction; (c) No vibration; (d) Diagonal vibration.

unreasonable vibration parameters. Although the roughness can be significantly reduced at this time, this result is not what we expected. Therefore, through detailed experimental and simulation research, the purpose of this paper is to find the best and reasonable vibration parameters (frequency and amplitude) to ensure that the roughness is effectively reduced and the graphics are not distorted. The core technology is to apply the DMD discrete pixel gap through the auxiliary effect of mechanical vibration. For unreasonable vibration, it will cause serious deformation of the exposed MLA, which will affect its imaging quality, optical efficiency, and other problems.

To determine the optimal vibration parameters, an array of nine micro-lens (3×3, each lens diameter: 380 μm) was made, with frequencies gradually increasing from 0-400. The corresponding displacement was characterized by measuring the central offset of the micro-lens and the corresponding roughness was measured, as shown in Fig. 5. It is evident that when the frequency is 50 Hz, the center shift of the micro-lens is the largest, which is due to the low frequency and high amplitude currently, leading to graphics distortion. At the frequency of 150 Hz, the roughness is the smallest, which is close to the simulation result of 160 Hz. As the frequency continues to increase, the roughness and lens central offset increase, this is because that higher frequencies result in smaller amplitudes and the resulting vibrations are insufficient to smear the discrete pixels and smooth the micro-lens surfaces. Therefore, the optimal vibration frequency was set as 150 Hz.

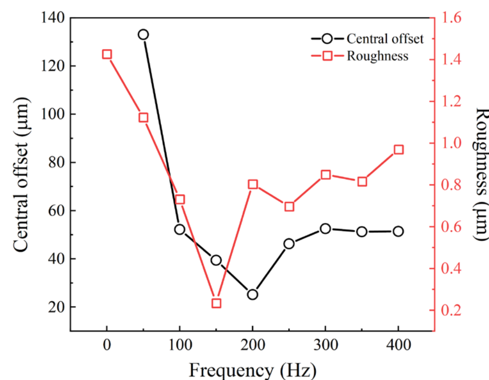

Fig. 5 Effect of vibration frequency on the central offset and roughness of micro-lens arrays by experiments.

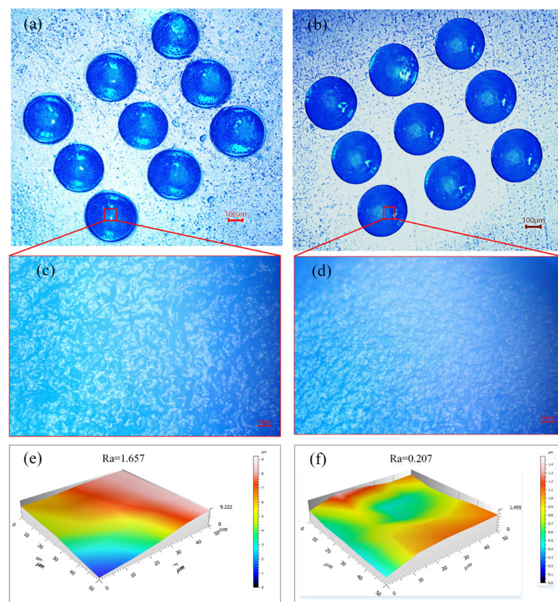

Fig. 6 Morphology and roughness of the micro-lens array before and after vibration. (a) The optical microscope morphology image before vibration. (b) The optical microscope morphology image after vibration. (c) A local magnification of any region of the micro-lens of (a). (d) A local magnification of any region of the micro-lens of (b). (e) A 3D view of the micro-lens roughness before vibration. (f) A 3D view of the micro-lens roughness after vibration.

Fig.6 showed the measured morphology and roughness of the micro-lens array. Fig.6(a) and 6(b) showed the optical microscope image of the measured micro-lens array before and after vibration, respectively. It can be obviously seen that the surface quality of the micro-lens after vibration is better than that before vibration. Fig. 6(c) and 6(d) are the local magnifications of Fig.6(a) and 6(b), respectively, which can be clearly seen that the surface of the micro-lens after vibration is smoother than that before vibration. To further characterize the surface quality of micro-lens quantitatively, 3D optical profilometer (PS50, Nanovea company) was used to measure the surface roughness, as depicted in Fig.6(e) and 6(f). The roughness measured represents the average roughness value of the measured middle region. Here, the selected middle region is an optional region on the MLA after processing, and there is no specificity. And because the middle region of the microlens is an important region that affects the quality of optical imaging, it is also an important reason to choose the middle region. In the actual experiment, several regions were also selected for measurement. Because the 3D optical profilometer used could not measure the roughness in a large range, the roughness measurement effect in the paper was finally presented in a small range (50 μm x 50 μm). The roughness values of each region are also very close. The experimental results showed that the surface roughness can be obviously reduced from 1.657 μm to 0.207 μm after applying vibration, a reduction of about 88%. Consequently, the surface quality of the micro-lens array can be significantly enhanced after the application of mechanical vibration, thereby validating the effectiveness of the proposed method.

4. Conclusions

In summary, we propose an efficient and cost-effective method to eliminate the effects of pixel quantization errors and to improve the surface quality of microstructure. By applying mechanical vibration to the projection objective, the DMD discrete pixel gap can be coated and the roughness is reduced by 88% while ensuring no distortion of the micro-lens. Compared with the existing DMD pixel error optimization methods, the mechanical vibration-assisted method ensures high fidelity and high surface quality of the micro-lens structure, which has significant industrial applications.

Acknowledgments

This work was supported by funding from the National Natural Science Foundation of China (62305001), Key Study and development program of Anhui Province (2022a05020008), Natural Science Foundation of Anhui Province (2308085MF210, 2008085QE258), Major Project of Natural Science Study in Universities of Anhui Province (2022AH040138), China Postdoctoral Science Foundation (2022M710175), Open Project of Special Display and Imaging Technology Innovation Center of Anhui Province (2022AJ05002), Research activities of postdoctoral researchers in Anhui Province (2023B707), the Anhui Province college young and middle-aged teachers training action project (JNFX2023015), the Anhui Polytechnic University Graduate Education Innovation Fund and the New Era Education Quality Project (Postgraduate Education).

References

[1] A. Camposeo A, L. Persano, M. Farsari, and D. Pisignano: Adv. Opt. Mater., 7, (2019) 1800419.

[2] M. Sieler, P. Schreiber, and A. Bräuer: Proc. SPIE, Vol. 8643, (2013) 86430B.

[3] S.H. Hong, J.S. Jang, and B. Javidi: Opt. Express, 12, (2004) 483.

[4] S. Kim, H. Kim, and S. Kang: Opt. Express, 12, (2004) 483.

[5] F. Zhang, Q. Yang, H. Bian, F. Liu, M. Li, X. Hou, and F. Chen: IEEE Photonic. Tech. L., 32, (2020) 1327.

[6] L. J. Wang, R. Sun, T. Vasile, Y. C. Chang, and L. Li: Anal. Chem., 88, (2016) 8302.

[7] L.J. Wang, Y.C. Chang, R. Sun, and L. Li: Biosens. Bioelectron., 87, (2017) 686.

[8] A. Hassanfiroozi, Y.P. Huang, B. Javidi, and H.P.D. Shieh: Opt. Express, 24, (2016) 8527.

[9] X.Q. Liu, L. Yu, S.N. Yang, Q.D. Chen, L. Wang, S. Juodkazis, and H.B. Sun: Laser & Photonics Reviews, 13, (2019) 1800272.

[10] S.I. Bae, K. Kin, S. Yang, K.W. Jang, and K.H. Jeong: Opt. Express, 28, (2020) 9082.

[11] X. Zhou, Y. Peng, R. Peng, X. Zeng, Y.A. Zhang, and T. Guo: ACS Appl. Mater. Interfaces, 8, (2016) 24248.

[12] L. Meng, Y. Zhang, X. Wan, C. Li, X. Zhang, Y. Wang, X. Ke, Z. Xiao, L. Ding, R. Xia, H.L. Yip, Y. Cao, and Y. Chen: Science, 361, (2018) 1094.

[13] Y. Xing, X.Y. Lin, L.B. Zhang, Y.P. Xia, H.L. Zhang, H.Y. Cui, S. Li, T.Y. Wang, H. Ren, D. Wang, H. Deng, and Q.H. Wang: Opto-Electron. Adv., 6, (2023) 220178.

[14] R.E. Alsaigh, R. Bauer, and M.P.J. Lavery: Opt. Express, 28, (2020) 31714.

[15] V. Grigaliūnas, A. Lazauskas, D. Jucius, D. Viržonis, B. Abakevičienė, S. Smetona, and S. Tamulevičius: Microelectron. Eng., 164, (2016) 23.

[16] J. Li, W. Wang, X. Mei, D. Hou, A. Pan, B. Liu, and J. Cui: ACS Appl. Mater. Interfaces, 12, (2020) 8870.

[17] T. Gissibl, S. Thiele, A. Herkommer, and H. Giessen: Nat. Photonics, 10, (2016) 554.

[18] H. Zhang, F. Yang, J. Dong, L. Du, C. Wang, J. Zhang, C.F. Guo, and Q. Liu: Nat. Commun., 7, (2016) 13743.

[19] Z. Xiong, H. Li, P. Kunwar, Y. Zhu, R. Ramos, S. Mcloughlin, T. Winston, Z. Ma, and P. Soman: Biofabrication, 11, (2019) 035005.

[20] P. Kunwar, Z. Xiong, Y. Zhu, H. Li, A. Filip, and P. Soman: Adv. Opt. Mater., 7, (2019) 900656.

[21] M. Kang, C. Han, and H. Jeon: Optica, 7, (2020) 1788.

[22] Y.M. Ha, I.B. Park, H.C. Kim, and S.H. Lee: Int. J. Precis. Eng. Man, 11, (2010) 335.

[23] J. Choi, G. Kim, W.S. Lee, W.S. Chang, and H. Yoo: Opt. Express, 30, (2022) 22487.

[24] J. Lee, H. Lee, and J. Yang: J. Mech. Sci. Tech, 32, (2018) 2209.

[25] R. Chen, H. Liu, H. Zhang, W. Zhang, J. Xu, W. Xu, and J. Li: Opt. Express, 25, (2017) 21958.

[26] S. Huang, L. Wang, Y. Zheng, F. Wang, and Y. Su, Appl. Phys. Express, 13, (2020) 116501.

[27] Y. Sun, H. Liu, J. Li, Z. Lu, Y. Zhang, and Y. Luo: Acta Photonica Sinic., 48, (2019) 0411002.

[28] S. Guo, Z. Lu, Z. Xiong, L. Huang, H. Liu, and J. Li: Opt. Lett, 46, (2021) 1377.

[29] Y. Zhang, J. Luo, Z. Xiong, H. Liu, L. Wang, Y. Gu, Z. Lu, J. Li, and J. Huang: Opt. Express, 27, (2019) 31956.

[30] Z. Huang, G. Shao, and L. Li: Prog. Mater. Sci., 131, (2023) 101020.

[31] L. Huang, C. Liu, H. Zhang, S. Zhao, M. Tan, M. Liu, Z. Jia, R. Zhai, and H. Liu: Opt. Laser Technol., 157, (2023) 108666.

(Received: October 22, 2023, Accepted May 15, 2024)